Nonlinear Control of Covid-19 Pandemic Based on the SIRD Model

Seyyed Mostafa Ghadami, Seyyed Masoud Seyyedi and
Rituraj Rituraj

Nonlinear control of Covid-19 pandemic based on the SIRD model

Seyyed Mostafa Ghadami
dept. of Electrical Engineering
Aliabad Katoul Branch, Islamic Azad
University
Aliabad Katoul, Iran
ghadami@aliabadiau.ac.ir

Seyyed Masoud Seyyedi
dept. of Mechanical Engineering
Aliabad Katoul Branch, Islamic Azad
University
Aliabad Katoul, Iran
s.masoudseyyedi@aliabadiau.ac.ir

R. Rituraj
Doctoral School of Applied Informatics
and Applied MathematicsObuda
University
Budapest, Hungary
rituraj88@stud.uni-obuda.hu

Abstract—**In the last month of 2019, a new version of Corona disease was observed in Wuhan (China) which is known as Covid-19. Several models have been proposed to predict disease treatment. The SIR model is considered one of the simplest models for the prediction of pandemic disease. This means susceptible (S), infected (I), and recovered (R) populations. The SIRD model is yet another method that includes one more equation, i.e., the number of deaths (D). This paper proposed a control law for the first time to prevent the progression of the disease. The proposed control law is based on the SIRD model that is determined using two methods, i.e., the input-state feedback linearization method and the input-output feedback linearization method for the nonlinear modeling of Covid-19. The goal of control in this model is to reduce the percentage or number of infected people and the number of deaths due to Covid-19 disease. Simulation results show that the feedback linearization methods can have positive results in a significant reduction in unfurl of Covid-19. Delay in quarantine of infected people and constant percentage of people who should be quarantined are investigated as two important parameters. Results show that the percentage of infected people decreases 96.3 % and the percentage of deaths decreases 93.6 % when delay in quarantine equals 7 weeks.**

Keywords—*COVID-19, SIRD Model, Pandemic, Feedback Linearization, Quarantine Management*

I. INTRODUCTION

COVID-19 is a contagious disease caused by a newly discovered coronavirus. Researchers have tried mathematical modeling of COVID-19. Already, there are several models for infectious diseases. In 1927, the SIR model was proposed by McKendrick and Kermack [1] It is a nonlinear system of ordinary differential equations (ODEs). Another model was introduced by Weston et al. [2] which is called the SIRD model. The SIRD model is also a nonlinear system of ODEs that can be written as follows [2]:

$$\dot{S} = -\beta SI/N \qquad (1)$$

$$\dot{I} = \frac{\beta SI}{N} - (\gamma_R + \gamma_D)I \qquad (2)$$
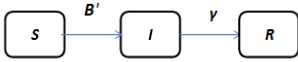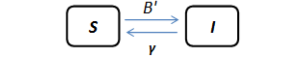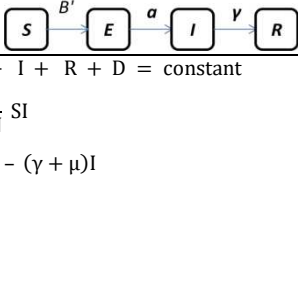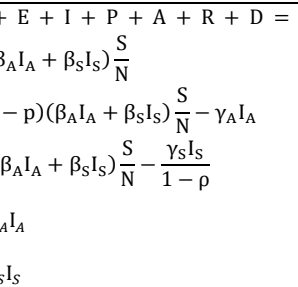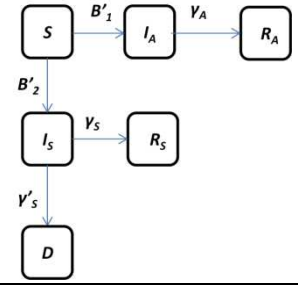
$$\dot{R} = \gamma_R I \qquad (3)$$

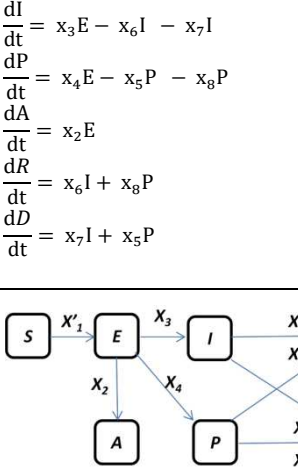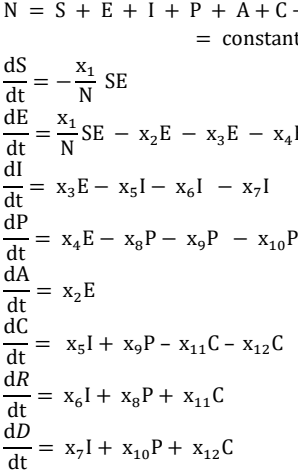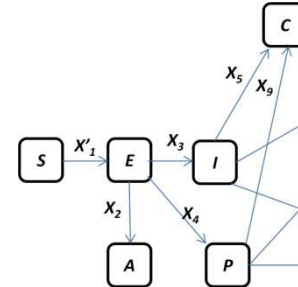$$\dot{D} = \gamma_D I \qquad (4)$$

A more complicated model is called the SIRASD model that is based on splitting the infected individuals into symptomatic and asymptomatic [3]. In 2010, Shabbir et al. [4] found an exact approach to a specific case of the SIR and Susceptible–Infected–Susceptible (SIS) disease models. Since the illness does not grant immunity against reinfection, the patients in the SIS model return to the susceptible community after treatment. Harko et al. [5] obtained an exact empirical solution to the SIR model in a parametric manner in 2014. They assumed that the death and birth rates were equal. A good review of the analytical and numerical solutions of different models has been provided by Ref. [5]. In 2017, Alasmawi et al. [6] studied Middle East respiratory syndrome coronavirus by an extending SEIR model. This consisted of five sets of population that included susceptible (S), infected (I), recovered (R), super-spreaders (P), and hospitalized (H). In 2020, Zareie et al. [7] locally model the coronavirus epidemic using the basic SIR model. They estimated a peak by the late March with over thousands of seven hundreds of confirmed cases. Sedaghat et al. [8] performed the sensitivity analysis on the predictive capability of the SIRD model. In 2020, Mahmoudi et al. [9] categorized high risk countries based on the spread rate of Covid-19. This was done using the principal component analysis method. In Wuhan, Toronto, and Italy, Xue et al. [10] used a similar SEIR type model for COVID-19. They used the MCMC optimization algorithm to find model coefficients. However, they only tested their model against two sets of clinical results. The SEIR-PAD model was introduced by Sedaghat et al. [11,12] using the extension of the SIR model. The SEIR-PAD model is the extension of the SEIR model considering the asymptomatic infected, super-spreader, and deceased individuals consisting various sets of differential equations. Table 1 includes the fundamental models of the pandemic [1,2,12]. Further advanced SIRD-based models and data-driven had been investigated in [13-21].

Table 1 Models of pandemic disease

Name of model	Equations and Flow chart
SIR (or xyz)	N = S + I + R = constant $\frac{dS}{dt} = -\frac{\beta}{N} SI$ $\frac{dI}{dt} = \frac{\beta}{N} SI - \gamma I$ $\frac{dR}{dt} = \gamma I$

Model	Equations
	$S \xrightarrow{B'} I \xrightarrow{\gamma} R$
SIS	$N = S + I = \text{constant}$ $\dfrac{dS}{dt} = -\dfrac{\beta}{N}SI + \gamma I$ $\dfrac{dI}{dt} = \dfrac{\beta}{N}SI - \gamma I$
	$S \underset{\gamma}{\overset{B'}{\rightleftarrows}} I$
SEIR	$N = S + E + I + R = \text{constant}$ $\dfrac{dS}{dt} = -\dfrac{\beta}{N}SI + \mu N - \mu S$ $\dfrac{dE}{dt} = \dfrac{\beta}{N}SI - (\mu + a)E$ $\dfrac{dI}{dt} = aE - (\gamma + \mu)I$ $\dfrac{dR}{dt} = \gamma I - \mu R$
	$S \xrightarrow{B'} E \xrightarrow{a} I \xrightarrow{\gamma} R$
SIRD	$N = S + I + R + D = \text{constant}$ $\dfrac{dS}{dt} = -\dfrac{\beta}{N}SI$ $\dfrac{dI}{dt} = \dfrac{\beta}{N}SI - (\gamma + \mu)I$ $\dfrac{dR}{dt} = \gamma I$ $\dfrac{dD}{dt} = \mu I$
SIRASD	$N = S + E + I + P + A + R + D = \text{constant}$ $\dfrac{dS}{dt} = -(\beta_A I_A + \beta_S I_S)\dfrac{S}{N}$ $\dfrac{dI_A}{dt} = (1-p)(\beta_A I_A + \beta_S I_S)\dfrac{S}{N} - \gamma_A I_A$ $\dfrac{dI_S}{dt} = p(\beta_A I_A + \beta_S I_S)\dfrac{S}{N} - \dfrac{\gamma_S I_S}{1-\rho}$ $\dfrac{dR_A}{dt} = \gamma_A I_A$ $\dfrac{dR_S}{dt} = \gamma_S I_S$ $\dfrac{dD}{dt} = \dfrac{\rho}{1-\rho}\gamma_S I_S$
	$N = S + E + I + P + A + R + D = \text{constant}$ $\dfrac{dS}{dt} = -\dfrac{x_1}{N}SE$ $\dfrac{dE}{dt} = \dfrac{x_1}{N}SE - x_2E - x_3E - x_4E$

Model	Equations
SEIR-PAD	$\dfrac{dI}{dt} = x_3E - x_6I - x_7I$ $\dfrac{dP}{dt} = x_4E - x_5P - x_8P$ $\dfrac{dA}{dt} = x_2E$ $\dfrac{dR}{dt} = x_6I + x_8P$ $\dfrac{dD}{dt} = x_7I + x_5P$
SEIR-PADC	$N = S + E + I + P + A + C + R + D = \text{constant}$ $\dfrac{dS}{dt} = -\dfrac{x_1}{N}SE$ $\dfrac{dE}{dt} = \dfrac{x_1}{N}SE - x_2E - x_3E - x_4E$ $\dfrac{dI}{dt} = x_3E - x_5I - x_6I - x_7I$ $\dfrac{dP}{dt} = x_4E - x_8P - x_9P - x_{10}P$ $\dfrac{dA}{dt} = x_2E$ $\dfrac{dC}{dt} = x_5I + x_9P - x_{11}C - x_{12}C$ $\dfrac{dR}{dt} = x_6I + x_8P + x_{11}C$ $\dfrac{dD}{dt} = x_7I + x_{10}P + x_{12}C$

The above results show that social distancing, quarantine, and isolation of infected populations support in controlling of an epidemic. As can be seen in the literature, none of them have examined the effects of control laws on infected individuals (I), or other populations. For the first time, we investigated the effects of a control law (such as quarantine) on the infected individuals. The aim is to prevent the spread of the epidemic.

II. MATHEMATICAL MODELING

Here, we propose a control law based on SIRD model (See Eqs. 1-4).

$$\dot{S} = -\beta SI/N \tag{5}$$

$$\dot{I} = \frac{\beta SI}{N} - (\gamma_R + \gamma_D)I - Iu(t) \tag{6}$$

$$\dot{R} = \gamma_R I \tag{7}$$

$$\dot{D} = \gamma_D I \tag{8}$$

where the total population N is considered as constant and can be written as

$$N = S + I + R + D = \text{constant} \tag{9}$$

In the SIRD model, γ_R, and γ_D , β are the, the recovery rate, the death rate, and transmission rate respectively. as. shown in Eq. (6), $u(t)$ can be interpreted as a control law such as quarantine of infected individuals (I). In the SIRD model, two variables are independent (i.e., S and I) and two variables dependent (R and D) on the infected individuals (I). Therefore, it is reasonable that $u(t)$ is added into equation. (2) for controlling infected individuals.

To present the effects of control laws on preventing the spread of epidemics, we use real data [8] as a case study. Table 2 represents the coefficients of the SIRD model [8].
In this table, removing rate (γ) and Re-production number (R_0) are defined as follows, respectively. For more details, see Ref. [8].

$$\gamma = \gamma_R + \gamma_D \tag{10}$$

$$R_0 = \beta / \gamma \tag{11}$$

Table 2: The coefficients of the SIRD model [8]

No. of days	Growth rate (β)	Recovery rate (γ_R)	Death rate (γ_D)	Removing rate (γ)	Reproduction number (R_0)
20	0.18311	0.01363	0.00435	0.01798	10.18
40	0.14507	0.03524	0.00215	0.03739	3.88
60	0.12943	0.02308	0.00156	0.02464	5.25
80	0.13963	0.04158	0.00137	0.04295	3.25
100	0.13399	0.03576	0.00154	0.0373	3.59
116[a]	0.15188	0.05501	0.00099	0.0560	2.71

The values of the parameters related to 116 days have been used in this study as the values of the model parameters are gradually modified over a period of 116 days.

III. DESIGN OF NONLINEAR CONTROLLER USING THE FEEDBACK LINEARIZATION METHOD

Feedback linearization is a suitable method for controller designing when there is a nonlinear model for the system. The main idea of this method is to convert nonlinear system dynamics into a linear system. State variables for coronavirus disease are defined as follows:

$$x_1 = S \text{ and } x_2 = I \tag{12}$$

Therefore, according to the mathematical model of disease treatment (i.e. Eqs. 5 and 6), f and g matrices can be determined as follows [13]:

$$\dot{x} = f(x) + g(x)u \tag{13}$$

Where

$$f = \begin{bmatrix} -\beta SI/N \\ \frac{\beta SI}{N} - (\gamma_R + \gamma_D)I \end{bmatrix} \text{ and } g = \begin{bmatrix} 0 \\ -I \end{bmatrix} \tag{14}$$

It can be applied the feedback linearization method because the conditions of linearly independent (controllability) and involutivity are established (See, Appendix A). Here, z_1 and z_2 The variables must be determined as follows:

$$z_1 = \ln(S) \text{ and } z_2 = -\frac{\beta I}{N} \tag{15}$$

Thus, the state equations can be rewritten as follows:

$$\dot{z}_1 = z_2 \tag{16}$$

And

$$\dot{z}_2 = \frac{\beta e^{z_1} z_2}{N} - (\gamma_R + \gamma_D)z_2 - z_2 u \tag{17}$$

1) Input-State Feedback Linearization Method
In to the first step, f and g matrices must be determined as follows [13]:

$$\dot{z} = f(z) + g(z)u \tag{18}$$

Where

$$f = \begin{bmatrix} z_2 \\ \frac{\beta e^{z_1} z_2}{N} - (\gamma_R + \gamma_D)z_2 \end{bmatrix} \text{ and } g = \begin{bmatrix} 0 \\ -z_2 \end{bmatrix} \tag{19}$$

In the second step, the control law can be obtained as follows:

$$u = \frac{1}{L_g L_f z_1}\left[v - L_f{}^2 z_1\right] , \tag{20}$$

$$L_f{}^2 z_1 = \frac{\beta e^{z_1} z_2}{N} - (\gamma_R + \gamma_D)z_2,$$

$$L_g L_f z_1 = -\frac{\beta}{N}$$
$$v = \ddot{z}_1 = -k_0 z_1 - k_1 \dot{z}_1$$

If the issue at hand is reference input tracking ($z_{1d}(t)$), or error of tracking ($e(t) = z_1(t) - z_{1d}(t)$), it is enough that v is selected by:

$$v = \ddot{z}_{1d} - k_0 e - k_1 \dot{e} \tag{21}$$

2) Input-Output Feedback Linearization Method
In the first step, the output must be selected. It is reasonable that infected individuals (I) are considered as output since the S, R and D variables can be controlled by the controlling of $I(t)$. Thus, we have:

$$y = h(z) = z_2 \tag{22}$$

In the second step, the derivation output, the control law can be obtained as follows:

$$u = \frac{1}{L_g y}\left[v - L_f y\right], \tag{23}$$

$$L_f y = \frac{\beta e^{z_1} z_2}{N} - (\gamma_R + \gamma_D)z_2,$$

$$L_g y = -\frac{\beta}{N},$$

$$v = \dot{y} = -k_0 y$$

In this case, it is enough that v is selected by:

$$v = \dot{y} - k_0 e \qquad (24)$$

IV. RESULTS AND DISCUSSION

In this section, the simulation results of the population of 50,000 people from Kuwait are examined according to the proposed model, in different situations, without applying the law of control (without quarantine) and with applying the control law (quarantine).

1) Validation

Here, to validate the simulation results, the written MATLAB code is employed to obtain the results of Ref. [12]. As shown in Fig. 1, the results are in outstanding agreement with those of Sedaghat et al. [12]. It should be mentioned that the results of Ref. [12] are without a control law (without quarantine). As it can be seen in Fig 1 adapted from Sedaghat et al. [12], over a period of ten months, in the worst situation, more than 13000 people will be infected with the COVID-19 and more than 800 people will die. Now, by applying the control law (quarantine) using the feedback linearization methods, we will evaluate the results.

2) Investigating Effect of Delay in Implementing the Control Law (Quarantine)

One of the important factors is the delay in applying the quarantine. If the expected quarantine rule is delayed for several weeks, the output can be expected to be delayed. On the other hand, if it is possible to apply the control law from the first week, then the disease will be controlled in the first weeks. The impact of delays in enforcing the control law is shown below. Fig. 2 presents variations in S, I, R, and D populations versus time in different values of delay. The figure shows that the number of infected individuals first increases, reaches a maximum value, and then decrease with time. The maximum value without quarantine is 13173, while it is12328, 5763, 1908 and 491 for delay values 13, 11, 9 and 7 weeks, respectively.
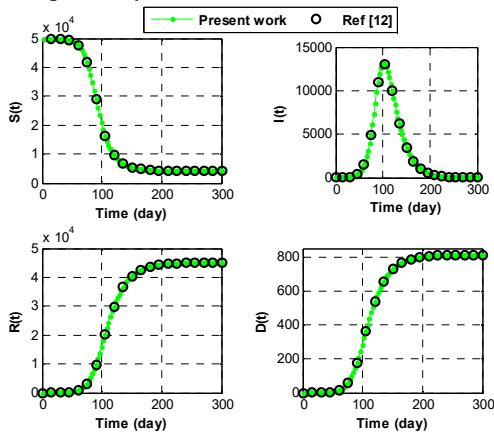

Fig. 1 Results comparison between given work

Also, the number of deaths decreases as the delay value decreases. The maximum number of deaths without quarantine is 810, while it is 753, 465, 187 and 52 for delay values 13, 11, 9 and 7 weeks, respectively. The calculations

discover that the number of deaths decreases from 810 to 52 people.

Fig. 3 shows the percentage of infected people who should be quarantined. This value is around 12.2%, 9.7%, 4.9% and 0% for delay value 7, 9, 11 and 13 weeks, respectively. The figure indicates that after 13 weeks, the percentage of infected people who should be quarantined is almost similar to that of those without quarantine. Fig. 4 demonstrates the share of S, I, R, and D in the total number of population for different values of delay. As it can be seen, for example, I increase from less than 1% to 4% when delay goes up from 7 to 13 weeks. Also, the number of deaths increased to almost one percent of the total population after 13 weeks of delay.
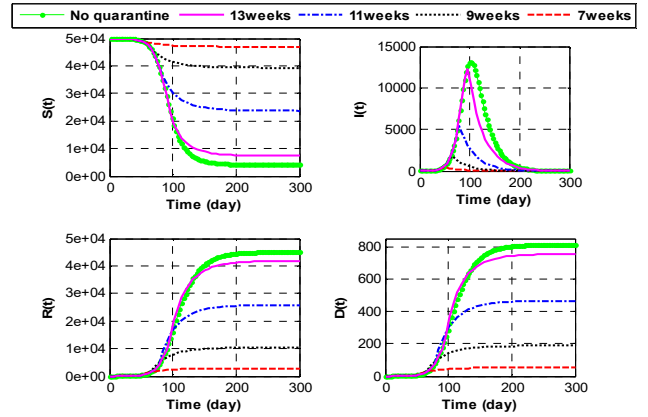

Fig. 2 Variations of S, I, R, and D population.s versus time in different values of delay
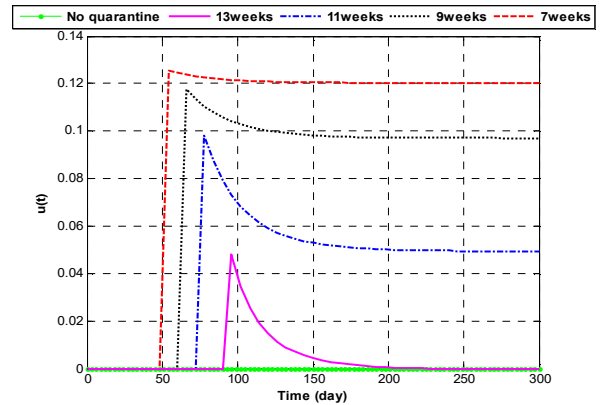

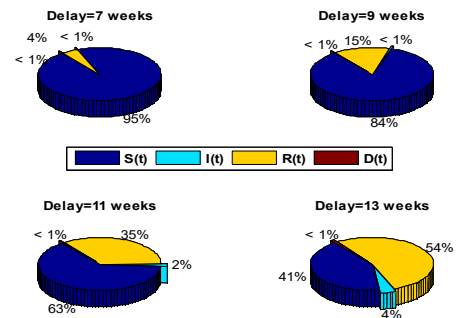Fig. 3 Percentage of infected people who should be quarantined

Fig. 4 Share of susceptible (S), infected (I), recovered (R) individuals and number of deaths (D) in the total population

You can see from the Figs. 2-4 that after a delay of about 13 weeks, the results are practically similar to situation without quarantine. This means that the quarantine of individuals has almost no effect on the outcome. The lower delay, the better the results, and therefore, a higher percentage should be quarantined.

3) Investigating the Effect of the Percentage of Quarantined People

Another important factor is the percentage of infected people who should be quarantined. As seen from Fig.3, after a short time, the control law (u) converges to a constant value. Therefore, the results of the fixed quarantine (u = constant) are examined below. Fig. 5 illustrates the effect of the percentage of infected people who should be quarantined (u) on the S, I, R and D populations. Here, the value of u is considered as constant. The figure shows that the maximum value of infected people (I) (which occurs after 14 weeks) decreases with increasing the u. Also, for example, the maximum values of I are 13172, 10145, 3945, 825, and 63 people, for $u = 0,1,4,7$ and 10%, respectively where $u = 0$ means without quarantine. The number of deaths (D) decreases as u increases. For example, the values of deaths are 810, 762, 560, 274, and 24 people, for $u = 0,1,4,7$ and 10%, respectively.
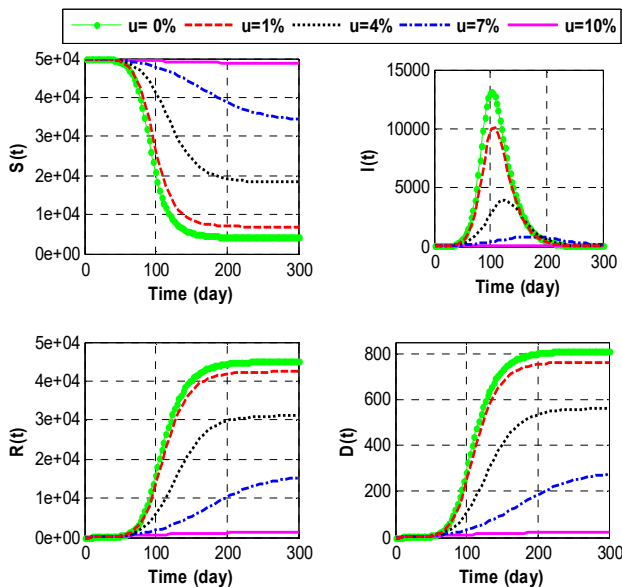

Fig. 5 Effect of the percentage of infected people who should be quarantined (u) on the S, I, R, and D populations

This indicates the importance the values of u. The results show that the number of death decrease 97% for $u = 10\%$. Fig. 6 represents a comparison between the average values of the S, I, R and D populations when u increases from 0 to 10%.

4) Simultaneous Study of the Effect of u and Delay in Starting Quarantine

Here, the effects of delay and u (that is considered as constant) are simultaneously examined. Results are shown in Figs. 7 and 8. You will notice that the higher the percentage of people who are quarantined with less delay, the lower the number of infected people and the number of deaths. According to Fig. 7, for example, the values of deaths are 706, and 364 people, when the value of u increases from 4% to 7% and delay decreases from 14 to 9 weeks. Also, for example, Fig. 8 shows that the infected population increases from 1%

to 4% when u decreases from 7% to 4% and delay increases from 9 to 14 weeks.
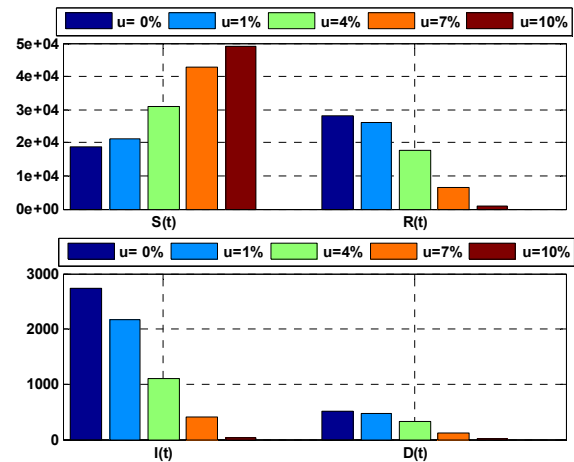

Fig. 6 Comparison between the values of the S, I, R, and D populations
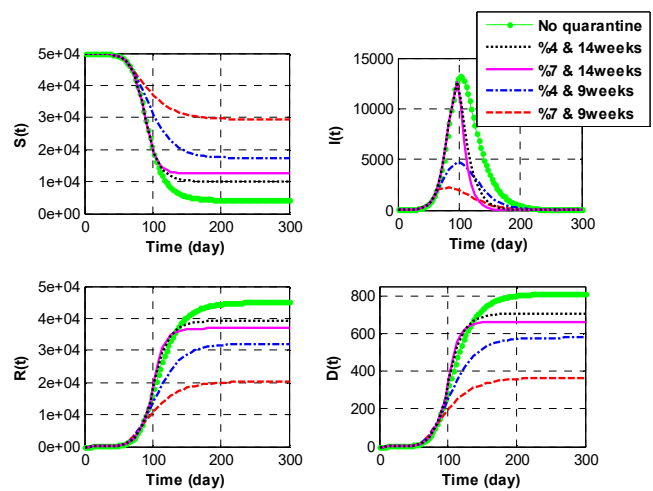

Fig. 7 Variations of S, I, R, and D populations versus time in different values of u and delay
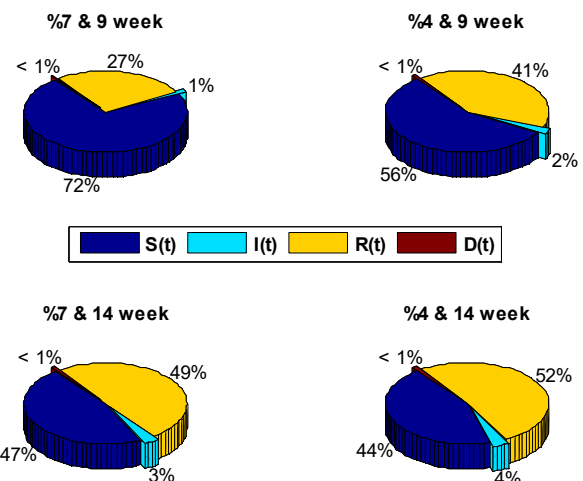

Fig. 8 Portion of S, I, R, D in the total number of population for different values of u and delay

5) Comparison Between Input-State Feedback Linearization Method and Input-Output Feedback Linearization Method

Fig. 9 presents the comparison between the input-state feedback linearization method and input-output feedback linearization method. As it can be seen, the results of the input-output feedback linearization method are better than that of input-state feedback linearization method in different values of delay. For example, the number of deaths are 757 and 52 people for the input-state and the input-output feedback linearization methods, respectively. This indicates that the second method is more effective as a control law.
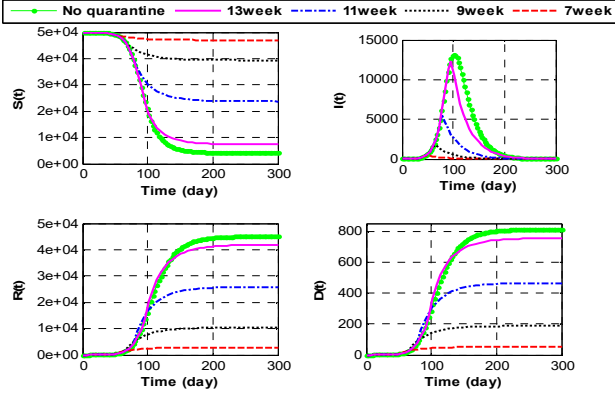
a) input-output feedback linearization method
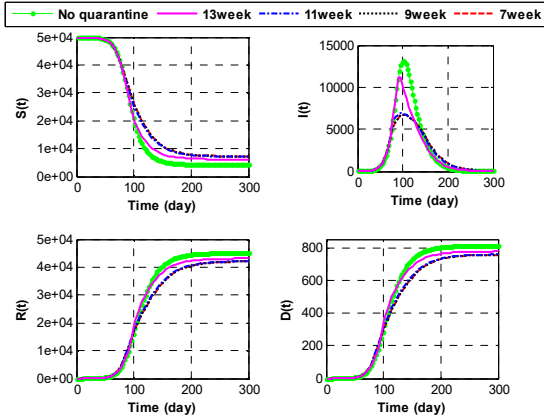
b) input-state feedback linearization method

Fig. 9 Variations of *S*, *I*, *R,* and *D* populations versus time for two methods

V. CONCLUSION

In this study, the SIRD model has been employed to investigate the effects of a control law (quarantine of people infected) on the propagation of Covid-19. For this purpose, real data on Covid-19 disease in Kuwait for 116 days were used. Then by enforcing the control law using the input-output feedback linearization method shows that controlling the propagation of Covid-19 has been very successful. The main results can be summarized as follows:

- Delay in quarantine of infected people and constant percentage of people who should be quarantined (u) are the important parameters.
- The maximum value of infected people without quarantine is 13173, while it is12328, 5763, 1908 and 491 for delay value 13, 11, 9 and 7 weeks, respectively. This means that the number of infected people decreases by 96.3 % and also, the number of deaths decreases from 810 to 52 people when delay equals 7 weeks (i.e. 93.6 % decreasing) (Fig. 2).

- The percentage of infected people who should be quarantined is approximately 12.2%, 9.7%, 4.9%, and 0% (at steady state) for delay values of 7, 9, 11, and 13 weeks, respectively (Fig. 3).
- The results show that the quarantine of infected people had almost no effect on the propagation of Covid-19 after 13 weeks' delay.
- The values of deaths are 810, 762, 560, 274, and 24 people, for $u = 0,1,4,7$ and 10%, respectively, i.e., 97% decreasing for $u = 10\%$ (Fig. 5).

The infected population increases from 1% to 4% when u decreases from 7% to 4% and delay increases from 9 to 14 weeks (Fig. 8). For future studies, a comparative analysis of the ensemble [22,23], tree-based [24], ANFIS [25], deep learning [26], artificial neural network [27] support vector machine [28], hybrid [29,30], clustering and classification [31], and other advanced statistics methods [32,33] is proposed for an insight into an optimal model with higher accuracy.

APPENDIX

Consider the nonlinear system adapted from [13] as follows.

$$\dot{x} = f(x,u) \tag{A.1}$$

The input-state linearization method solves this problem in two steps. In the first step, a diffeomorphism $z = z(x)$ and a control law $u = u(x,v)$ must be obtained where model of nonlinear system convert into model of linear time invariant system in the form as follows [13].

$$\dot{z} = Az + Bv \tag{A.2}$$

Where

$$A = \begin{bmatrix} 0 & 1 & 0 & \vdots & 0 \\ 0 & 0 & 1 & \vdots & 0 \\ & \vdots & & \vdots & \vdots \\ 0 & 0 & 0 & \vdots & 1 \\ 0 & 0 & 0 & \vdots & 0 \end{bmatrix} \quad \text{and} \quad B = \begin{bmatrix} 0 \\ \vdots \\ 0 \\ 1 \end{bmatrix} \tag{A.3}$$

In the second step pole placement method is used to form the input *v.* Fig. A.1 which is adapted from [13] shows the closed-loop system under the input-state feedback linearization method. In this figure you can see that there were two feedback loops. The inner loop is for input-state relationship linearization while the external loop is to achieve stability of the closed-loop dynamics. This indicates that u control input is a combination of a nonlinear elimination part and a linear compensation part. Consider the affine, SISO and nonlinear system as follows adapted from [13].

$$\dot{x} = f(x) + g(x)u \tag{A.4}$$

and,

$$y = h(x) \tag{A.5}$$

where, f and g are smooth vector fields on $R^{(n)}$ and $x = [x_1 \ x_2 \ ... \ x_n]$. Also, $h(x)$ is the output of the system as a scalar function. The Lie derivative is now defined as follows.

$$L_f h(x) = \frac{\partial h}{\partial x} \cdot f(x) \tag{A.6}$$

Therefore, higher-order derivatives are obtained as follows:

$$L_f^{(i)}h(x) = L_f(L_f^{(i-1)}h(x)) \tag{A.7}$$

On the other hand,

$$L_g L_f \, h(x) = L_g\left(\frac{\partial h}{\partial x}.f(x)\right) = \frac{\partial(\frac{\partial h}{\partial x}.f(x))}{\partial x}.g(x) \tag{A.8}$$
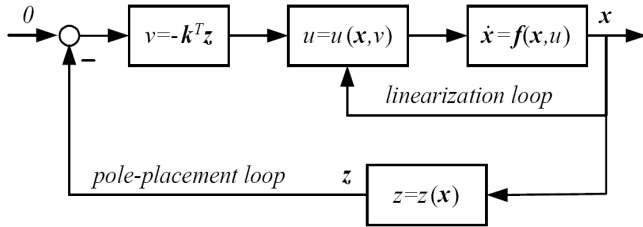

Fig. A1 Closed-loop system under input-state linearization method

REFERENCES

[1] Kermack, W.O. and McKendrick, A.G., 1927. A contribution to the mathematical theory of epidemics. Proceedings of the royal society of london. Series A, Containing papers of a mathematical and physical character, 115(772), pp.700-721.

[2] Roda, W.C., Varughese, M.B., Han, D. and Li, M.Y., 2020. Why is it difficult to accurately predict the COVID-19 epidemic? Infectious Disease Modelling, 5, pp.271-281.

[3] Bastos, S.B. and Cajueiro, D.O., 2020. Modeling and forecasting the early evolution of the Covid-19 pandemic in Brazil. *Scientific Reports*, *10*(1), pp.1-10.

[4] Shabbir, G., Khan, H. and Sadiq, M.A., 2010. A note on Exact solution of SIR and SIS epidemic models. *arXiv preprint arXiv:1012.5035*.

[5] Harko, T., Lobo, F.S. and Mak, M.K., 2014. Exact analytical solutions of the Susceptible-Infected-Recovered (SIR) epidemic model and of the SIR model with equal death and birth rates. *Applied Mathematics and Computation*, *236*, pp.184-194.

[6] Alasmawi, H., Aldarmaki, N. and Tridane, A., 2017. Modeling of a super-spreading event of the MERS-corona virus during the Hajj season using simulation of the existing data. *Int. J. of Statistics in Medical and Biological Research*, *1*(1), pp.24-30.

[7] Zareie, B., Roshani, A., Mansournia, M.A., Rasouli, M.A. and Moradi, G., 2020. A model for COVID-19 prediction in Iran based on China parameters. *MedRxiv*.

[8] Sedaghat, A., et al., 2020. Sensitivity Analysis on Predictive Capability of SIRD Model for Coronavirus Disease (COVID-19). *medRxiv*.

[9] Mahmoudi, M.R., Heydari, M.H., Qasem, S.N., Mosavi, A. and Band, S.S., 2021. Principal component analysis to study the relations between the spread rates of COVID-19 in high risks countries. *Alexandria Engineering Journal*, *60*(1), pp.457-464.

[10] Xue, L., Jing, S., Miller, J.C., Sun, W., Li, H., Estrada-Franco, J.G., Hyman, J.M. and Zhu, H., 2020. A data-driven network model for the emerging COVID-19 epidemics in Wuhan, Toronto and Italy. *Mathematical Biosciences*, *326*, p.108391.

[11] Sedaghat, A., et al., 2020, COVID-19 (Coronavirus Disease) Outbreak Prediction Using a Susceptible-Exposed-Symptomatic Infected-Recovered-Super Spreaders-Asymptomatic Infected-Deceased-Critical (SEIR-PADC) Dynamic Model. In *2020 IEEE 3rd International Conference and Workshop in Óbuda on Electrical and Power Engineering (CANDO-EPE)* (pp. 000275-000282). IEEE.

[12] Sedaghat, A., Oloomi, S.A.A., Malayer, M.A. and MOSAVI, A., 2020. Trends of COVID-19 (Coronavirus Disease) in GCC Countries using SEIR-PAD Dynamic Model. *medRxiv*.

[13] Slotine, Jean-Jacques E., and Weiping Li. Applied nonlinear control. Vol. 199, no. 1. Englewood Cliffs, NJ: Prentice hall, 1991.

[14] Sedaghat, A., et al., 2020, November. Modeling and sensitivity analysis of coronavirus disease (COVID-19) outbreak prediction. In 2020 IEEE 3rd International Conference and Workshop in Óbuda on Electrical and Power Engineering (CANDO-EPE) (pp. 000261-000266). IEEE.

[15] Sedaghat, A., et al., 2020, Predicting COVID-19 (Coronavirus Disease) Outbreak Dynamics Using SIR-based Models: Comparative Analysis of SIRD and Weibull-SIRD. In 2020 IEEE 3rd International Conference and Workshop in Óbuda on Electrical and Power Engineering (CANDO-EPE) (pp. 000283-000288). IEEE.

[16] Ardabili, S., et al., 2020, Coronavirus disease (COVID-19) global prediction using hybrid artificial intelligence method of ANN trained with Grey Wolf optimizer. In 2020 IEEE 3rd International Conference and Workshop in Óbuda on Electrical and Power Engineering (CANDO-EPE) (pp. 000251-000254). IEEE.

[17] Sedaghat, A., et al., 2020, Coronavirus (COVID-19) outbreak prediction using epidemiological models of Richards Gompertz Logistic Ratkowsky and SIRD. In 2020 IEEE 3rd International Conference and Workshop in Óbuda on Electrical and Power Engineering (CANDO-EPE) (pp. 000289-000298). IEEE.

[18] Sedaghat, A., et al., 2020, Predicting Trends of Coronavirus Disease (COVID-19) Using SIRD and Gaussian-SIRD Models. In 2020 IEEE 3rd International Conference and Workshop in Óbuda on Electrical and Power Engineering (CANDO-EPE) (pp. 000267-000274). IEEE.

[19] Tabrizchi, H., et al., 2021, Densely Connected Convolutional Networks (DenseNet) for Diagnosing Coronavirus Disease (COVID-19) from Chest X-ray Imaging. In 2021 IEEE International Symposium on Medical Measurements and Applications (MeMeA) (pp. 1-5). IEEE.

[20] Tabrizchi, H., 2022. Deep Learning Applications for COVID-19: A Brief Review. In International Conference on Global Research and Education (pp. 117-130). Springer, Singapore.

[21] Tabrizchi, H., 2020, Rapid COVID-19 diagnosis using deep learning of the computerized tomography Scans. In 2020 IEEE 3rd International Conference and Workshop in Óbuda on Electrical and Power Engineering (CANDO-EPE) (pp. 000173-000178). IEEE.

[22] Mosavi, A., Golshan, M., Janizadeh, S., Choubin, B., Melesse, A.M. and Dineva, A.A., 2020. Ensemble models of GLM, FDA, MARS, and RF for flood and erosion susceptibility mapping: a priority assessment of sub-basins. Geocarto International, pp.1-20.

[23] Ardabili, S., et al., 2019,. Advances in machine learning modeling reviewing hybrid and ensemble methods. In International Conference on Global Research and Education (pp. 215-227). Springer, Cham.

[24] Band, S.S., et al., 2020. Flash flood susceptibility modeling using new approaches of hybrid and ensemble tree-based machine learning algorithms. Remote Sensing, 12(21), p.3568.

[25] Rezakazemi, M., et al., 2019. ANFIS pattern for molecular membranes separation optimization. Journal of Molecular Liquids, 274, pp.470-476.

[26] Band, S.S.,et al., 2020. Novel ensemble approach of deep learning neural network (DLNN) model and particle swarm optimization (PSO) algorithm for prediction of gully erosion susceptibility. Sensors, 20(19), p.5609.

[27] Sadeghzadeh, M., et al., 2020. Prediction of thermo-physical properties of TiO2-Al2O3/water nanoparticles by using artificial neural network. Nanomaterials, 10(4), p.697.

[28] Karballaeezadeh, N., et al., 2019. Prediction of remaining service life of pavement using an optimized support vector machine (case study of Semnan–Firuzkuh road). Engineering Applications of Computational Fluid Mechanics, 13(1), pp.188-198.

[29] Choubin, B., et al., 2019. Earth fissure hazard prediction using machine learning models. Environmental research, 179, p.108770.

[30] Emadi, M., et al., 2020. Predicting and mapping of soil organic carbon using machine learning algorithms in Northern Iran. Remote Sensing, 12(14), p.2234.

[31] Torabi, M., et al., 2019. A Hybrid clustering and classification technique for forecasting short - term energy consumption. Environmental progress & sustainable energy, 38(1), pp.66-76.

[32] Maleki, M., et al., 2022. Skewed Auto-Regressive Process with Exogenous Input Variables: An Application in the Administered Vaccine Doses on Covid-19 Spread. Fractals.

[33] Mahmoudi, M.R. and Mosavi, A., 2022. Cyclocopula Technique to Study the Relationship between two Cyclostationary time Series with Fractional Brownian Motion Errors. Fractals.